Journal of Inorganic Biochemistry 204 (2020) 110986

Contents lists available at ScienceDirect

Journal of Inorganic Biochemistry

journal homepage: www.elsevier.com/locate/jinorgbio

Formation and kinetic studies of manganese(IV)-oxo porphyrins: Oxygen atom transfer mechanism of sulfide oxidations

Seth Klaine, Fox Bratcher, Charles M. Winchester, Rui Zhang*

Department of Chemistry, Western Kentucky University, 1906 College Heights Blvd #11079, Bowling Green, KY 42101-1079, United States of America

ARTICLE INFO

Keywords:
Manganese-oxo
Porphyrin
Sulfide oxidation
Kinetics
Visible light

ABSTRACT

Visible light irradiation of photo-labile porphyrin-manganese(III) chlorates or bromates (**2**) produced manganese (IV)-oxo porphyrins [Mn^{IV}(Por)(O)] (Por = porphyrin) (**3**) in three porphyrin ligands. The same oxo species **3** were also formed by chemical oxidation of the corresponding manganese(III) precursors (**1**) with iodobenzene diacetate, i.e. $PhI(OAc)_2$. The systems under study include 5,10,15,20-tetra(pentafluorophenyl)porphyrin-manganese(IV)-oxo (**3a**), 5,10,15,20-tetra(2,6-difluorophenyl)porphyrin-manganese(IV)-oxo (**3b**), and 5,10,15,20-tetramesitylporphyrin-manganese(IV)-oxo (**3c**). As expected, complexes **3** reacted with thioanisoles to produce the corresponding sulfoxides and over-oxidized sulfones. The kinetics of oxygen atom transfer (OAT) reactions of these generated **3** with aryl sulfides were studied in CH_3CN solutions. Second-order rate constants for sulfide oxidation reactions are comparable to those of alkene epoxidations and activated C—H bond oxidations by the same oxo species **3**. For a given substrate, the reactivity order for the manganese(IV)-oxo species was **3a** > **3b** > **3c**, consistent with expectations on the basis of the electron-withdrawing capacity of the porphyrin macrocycles. Free-energy Hammett analyses gave near-linear correlations with σ values, indicating no significant positive charge developed at the sulfur during the oxidation process. The mechanistic results strongly suggest [Mn^{IV}(Por)(O)] reacts as a direct OAT agent towards sulfide substrates through a manganese(II) intermediate that was detected in this work. However, an alternative pathway that involves a disproportionation of **3** to form a higher oxidized manganese(V)-oxo species may be significant when less reactive substrates are present. The competition product studies with the Hammett correlation plot confirmed that the observed manganese(IV)-oxo species is not the true oxidant for the sulfide oxidations catalyzed by manganese(III) porphyrins with $PhI(OAc)_2$.

1. Introduction

Catalytic oxidation is one of most important processes conducted daily on a large scale for the production of valuable chemicals, remediation of pollutants, and the production of energy [1–3]. In natural and synthetic oxidation catalysts, high-valent transition metal-oxo transients are typically involved as the oxygen atom transfer (OAT) intermediates. [4–6] In cytochrome P450 enzymes and heme-containing peroxidase and catalase enzymes, for example, the high-valent iron(IV)-oxo porphyrin radical cations, biologically termed compound I, are the primary oxidant [7,8]. The one-electron reduced form porphyrin-iron(IV)-oxo intermediates, commonly called compound II, also act as reactive species, [9,10] in particular in one electron-transfer oxidation reactions such as C—H activation and hydride-transfer reactions. [11]

In this context, extensive efforts have been directed to metalloporphyrins as P450s models, and a variety of active metal-oxo species were produced and characterized to elucidate the oxidation mechanisms. [4,12] In particular, manganese-oxo intermediates are among the more reactive oxidizing transition metal derivatives. Nature uses Mn-oxo species in the production of oxygen in photosystem II in plants. [13] A variety of manganese-oxo species are employed catalytically in applied syntheses [14–19] in which highly reactive porphyrin-manganese(V)-oxo derivatives [20–25] are proposed intermediates in catalytic processes. In addition to these manganese(V) porphyrins, unusual *trans*-dioxomanganese(V) porphyrins were also synthesized and characterized, which showed pH-dependent reactivities towards typical substrates. [26] The one-electron reduced manganese(IV)-oxo porphyrins

Abbreviations: Por, porphyrin; TMP, 5,10,15,20-tetramesityphenylporphyrin; TDFPP, 5,10,15,20-tetrakis(2,6-difluorophenyl)porphyrin; TPFPP, 5,10,15,20-tetrakis (pentafluorophenyl)porphyrin; $PhI(OAc)_2$, iodobenzene diacetate; OAT, oxygen atom transfer; LFP, laser flash photolysis

* Corresponding author.
E-mail address: rui.zhang@wku.edu (R. Zhang).

https://doi.org/10.1016/j.jinorgbio.2019.110986
Received 25 October 2019; Received in revised form 27 December 2019; Accepted 28 December 2019
Available online 31 December 2019

have also been prepared and characterized by their unique UV–vis absorption spectra and other spectroscopic methods including electron paramagnetic resonance (EPR), infrared (IR), and resonance Raman spectroscopies. [27–31] However, the well-characterized manganese (IV)-oxo derivatives are less investigated in view of their low reactivity, and unlikely serve as major oxidant in the catalytic oxidations. Very recently, unusually high reactivities of manganese(IV)-oxo porphyrins were reported in the C—H bond activation of hydrocarbons to afford the halogenated products. [32] Of note, kinetic studies of the reactivity of manganese(IV)-oxo derivatives are rather limited [33] particularly on the oxidation of compounds with heteroatoms such as sulfides.

Our group has aimed at understanding the energetics of oxidation reactions catalyzed by synthetic metalloporphyrins with a focus on reactivity of the important high-valent metal-oxo intermediates. Our particular interest in this area is to develop photochemical methods to generate and study reactive metal-oxo species in their OAT reactions. [34] Photochemical reactions are intrinsically advantageous because activation is obtained by the absorption of a photon, which leaves no residue; whereas most chemical methods involve the use of toxic and polluting reagents. As a general strategy for the generation of reactive species, the photochemical approach can provide much higher temporal resolution than those of the fastest mixing experiments, which is essential to detect the highly reactive transients. [34–36] For examples, laser flash photolysis (LFP) techniques have been successfully introduced for generation and kinetic studies of a variety of high-valent transition metal-oxo species supported by porphyrin ligands. [23,34–39] The photo-induced ligand cleavage and photo-disproportionation reactions were able to generate the highly reactive corrole-iron(V)-oxo intermediates that have not been detected before by other methods. [40,41] By extension, we applied photo-induced ligand cleavage reactions to produce *trans*-dioxo-ruthenium(VI) porphyrins [42,43] as well as a putative ruthenium(V)-oxo species [44] that was also found in a photo-disproportionation of the *bis*-porphyrin-ruthenium(IV) μ-oxo dimer. [45] Recently, we reported visible light-induced formation of iron(IV)-oxo porphyrin radical cations or iron(IV)-oxo porphyrins, controlled by the electronic structure of porphyrin ligands. [46,47] We also discovered a new photo-generation of manganese(V)-oxo corroles by visible light irradiation of photo-labile manganese(IV) bromate or nitrite precursors. [48,49] In this work, we describe our progress on photochemical generation of manganese(IV)-oxo porphyrins in three systems that can also be formed by chemical oxidations (Scheme 1). We report rate constants for the OAT reactions of porphyrin-manganese(IV)-oxo species with thioanisoles in acetonitrile solutions. The kinetic and spectral studies provide mechanistic insights as to the reaction pathways of the manganese(IV)-oxo intermediates in the sulfide oxidations.

2. Experimental

2.1. Materials and instruments

All commercial reagents were of the best available purity and were used as supplied unless otherwise specified. Acetonitrile was obtained from Sigma Aldrich (HPLC grade) and use as such. All organic substrates for kinetic studies were passed through a flash chromatography column of active alumina (Grade I) before use. The pyrrole for porphyrin synthesis was freshly distilled before use. 5,10,15,20-Tetrakis (pentafluorophenyl)porphyrin free ligand, [H_2(TPFPP)](**a**), 5,10,15,20-tetrakis(2,6-difluororophenyl)porphyrin, H_2(TDFPP)(**b**), and 5,10,15,20-tetramesitylporphyrin, H_2(TMP)(**c**), were prepared according to known methods. [50] All manganese(III) chloride complexes Mn^{III}(Por)Cl (**1a-c**; Por = porphyrin) used in this work were prepared by the literature-reported method [51] and characterized by UV–vis and ^{1}H NMR, matching those reported.

UV–vis spectra were conducted on an Agilent 8454 diode array spectrometer using standard 1.0-cm quartz cuvettes. ^{1}H NMR (Nuclear Magnetic Resonance) was performed on a JEOL ECA-500 MHz spectrometer at 298 K with tetramethylsilane (TMS) as the internal standard. Visible light was produced from a SOLA SE II light engine (Lumencor) configured with a liquid light guide (6–120 W). Kinetic measurements were performed on a stopped-flowed rapid mixing system (Applied Photophysics SX-20) using standard 1.0-cm quartz cuvettes. Gas chromatography-mass spectrometry (GC–MS) analysis were performed on an Agilent GC7820A/MS5977B, coupled with an auto sample injector using an Agilent DB-5 or Scientific *J* &W capillary columns. Electrospray ionization-mass spectroscopy (ESI-MS) data was collected using an Agilent 500 LC-MS Ion Trap System.

2.2. General procedure for synthesis of manganese(IV)-oxo porphyrins

Axial ligand exchange of the porphyrin complexes Mn^{III}(Por)Cl (**1**) with excess of Ag(ClO_3) or Ag(BrO_3) in CH_3CN or CH_2Cl_2 gave the corresponding chlorate or bromate complexes [Mn^{III}(Por)(XO_3)] (X = Cl or Br) (**2**), which were photo-labile and subsequently used for photochemical reactions. The solution of **2** with concentration of ca. 1.0×10^{-5} M was irradiated with visible light from a SOLA engine (output power 120 W) at ambient temperature. The formation of manganese(IV)-oxo porphyrin (**3**) was complete in the range of 3 to 5 s, as monitored by UV–vis spectroscopy. The photo transformation is characterized by a distinct UV–vis absorption changes, and

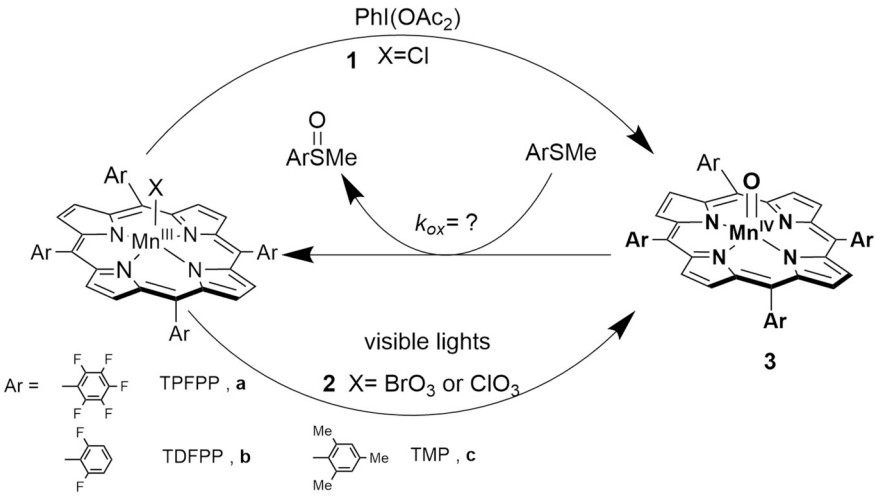

Scheme 1. Photochemical and chemical generation of porphyrin-manganese(IV)-oxo derivatives and kinetics of their sulfide oxidations

accompanied by the well-anchored isosbestic points. In each case, the resulting species **3** display sharper, stronger, blue-shifted Soret bands and Q bands that are characteristic for the corresponding porphyrin-manganese(IV)-oxo derivatives. Following our previous work, [52] the same [Mn^{IV}(Por)(O)] were also produced by chemical oxidation of precursors **1** with $PhI(OAc)_2$ (10 to 15 equiv.) as the sacrificial oxidant, and the time-resolved absorption spectra exhibited same characteristic features.

2.3. Stoichiometric sulfide oxidations

Solutions of **3** (20 μM) in CH_3CN (5 mL) were prepared as above, and the estimated yield of **3** determined by UV–vis spectroscopy was > 95%. To these were added excess thioanisole such that the final substrate concentration was 0.1 M. The mixtures were stirred for 5 to 10 min until the reaction was complete (monitored by UV–vis spectroscopy). The samples were filtered through an alumina column to remove the porphyrin complex and analyzed by GC–MS with an internal standard (1, 2, 4-trichlorobenzene), which was shown to be stable to the oxidation conditions in control reactions. Products including sulfoxides and sulfones from the over oxidation were identified by GC–MS. The yields of products were determined relative to standard using predetermined response factors.

2.4. Kinetic studies of manganese(IV)-oxo porphyrins

Reactions of high-valent porphyrin-manganese(IV)-oxo species with excess amounts of organic substrates were conducted in a stopped-flow unit (SX-20) at 23 ± 2 °C. The sequential three-syringe stopped-flow apparatus (SX-20) and associated computer system were from Applied Photophysics (UK). For a total of 400 μL/shot into a flow cell with 1 cm light path, the fastest time for mixing two solutions and recording the first data point was ca. 1 ms. Manganese(IV)-oxo porphyrins **3** (> 90% yield) was prepared in CH_3CN by reacting manganese(III) precursors **1** with 10 equiv. of $PhI(OAc)_2$. After a delay of 1 to 5 s, the resulting solution of species **3** was then mixed with another solution containing substrate in large excess (> 100 equiv). The rates of the reactions which represented the rates of oxo group transfer from high-valent iron (IV)-oxo **3** to sulfides were monitored by the decay of the Soret band at 420 to 425 nm of the high-valent manganese(IV)-oxo species. Rate constants for reactions with substrates are determined from kinetic measurements with varied concentrations of substrate. The kinetic traces at λ_{max} of the Soret band displayed good pseudo-first-order behavior with over four half-lives, and the data was solved to give pseudo-first-order observed rate constants, k_{obs}. Plots of these values against the concentration of substrate were linear in all cases. The second-order rate constants for reactions of the oxo species **3** with the organic substrates were solved according to Eq. (1), where k_0 is a background rate constant found in the absence of substrate, k_{ox} is the second-order rate constant for oxidation reaction with the substrate, and [Sub] (Sub = substrate) is the concentration of substrate. All second-order rate constants are averages of 2–3 determinations consisting of independent kinetic measurements. Errors in the rate constants were weighted at 2σ.

$$k_{obs} = k_0 + k_{ox}[\text{Sub}] \quad (1)$$

2.5. General procedure for catalytic sulfoxidations

Unless otherwise indicated, all catalytic reactions were typically carried out in the presence of a small amount of H_2O (4.5 μL) with 1 μmol of catalyst (0.2 mol%), 0.5 mmol of organic substrate and 1.5 equivalent of $PhI(OAc)_2$ (0.75 mmol) in 2 mL of methanol at 23 °C. Aliquots of the reaction solution at constant time interval were analyzed by GC/MS to determine the conversions, formed products and yields with an internal standard. All reactions were run 2 to 3 times, and the data reported represent the average of these reactions. Since the sulfoxidation reactions were not affected by molecular oxygen, all the reactions presented in Table 2 were performed in air.

2.6. Competition and Hammett correlation studies

A CH_3OH solution containing equal amounts of two substrates, e.g. thioanisole (0.2 mmol) and substituted thioanisoles (0.2 mmol), manganese(III) porphyrin catalyst (1 μmol) and an internal standard of 1,2,4-trichlorobenzene (0.1 mmol) was prepared (final volume = 0.5 mL). $PhI(OAc)_2$ (0.1 mmol) as the limiting reagent, was added and the mixture was stirred at ambient temperature (23 ± 2 °C) in the presence of a small amount of H_2O (4.5 μL) for 10 to 20 min. Relative rate ratios for catalytic oxidations were determined by GC based on the amounts of sulfoxide products as measured against an internal standard. In this work, all the catalytic sulfoxidations proceeded with good yields (> 95%), mass balance (> 95%), and in all cases no sulfones were detected. Thus, the ratio of product formation should reasonably reflect the relative sulfide reactivity towards the corrole-manganese-catalyzed oxidations.

3. Results and discussion

3.1. Formation of [Mn^{IV}(Por)(O)] and stoichiometric sulfide oxidations

As shown in Scheme 1, three tetraarylporphyrin–manganese systems that encompass the different electron demanding ligands were comparatively studied in this work. All ligand systems (**a-c**) are generally considered as sterically encumbered porphyrins due to the presence of relatively large substituents on the *ortho* positions of the *meso* phenyl groups, which will prevent the unwanted μ-oxo dimer formation. Among the macrocyclic ligands, tetrakis(pentafluorophenyl)porphyrin (TPFPP) is most electron-demanding ligand and 5,10,15,20-tetramesitylporphyrin (TMP) is least, and their metal complexes are among the more widely studied.

Axial ligand exchange of the porphyrin complexes (**1**) with excess $Ag(ClO_3)$ in CH_3CN gave the corresponding chlorate complexes [Mn^{III}(Por)(ClO_3)] (**2**), and their formation was confirmed by UV–vis spectra (Fig. S1 in the Supplementary information). Irradiation of the chlorate complex **2a** [Mn^{III}(TPFPP)(ClO_3)] in CH_3CN with visible light using a SOLA engine (output power of 120 W) resulted in changes in the absorption spectra with isosbestic points at 550, 442, 390 and 320 nm (Fig. 1A). Over a time period of 5 s, **2a** was converted to a new species **3a** that displayed a blue-shifted and stronger Soret band at 420 nm and Q-band at 540 nm. Similarly, irradiation of bromate complexes [Mn^{III}(TPFPP)(BrO_3)] also formed same products **3** with higher efficiency as reflected by faster formation with lower-power of visible light (data not shown). The photo-generated **3a** was metastable with a half-lifetime of ca. 5 min, and can be further characterized by ESI-MS. As shown in Fig. 1A (inset), the ESI-MS spectrum (positive mode) exhibited a prominent peak at a mass-to-charge ratio (*m/z*) of 1043, matching the calculated $[M + H]^+$ of [Mn(TPFPP)(O)]. When **3a** decayed, the prominent peak was shifted from 1043 to 1027 corresponding to $[Mn(TPFPP)]^+$. Accordingly, **3a** was assigned as [Mn^{IV}(TPFPP)(O)] on the basis of its distinct UV–vis absorption and ESI-MS. Control experiments showed that no species **3a** was formed in the absence of light. The use of the non-coordinating solvents such as CH_2Cl_2 gave similar results (data not shown). However, no formation of **3** was observed in CH_3OH solution or in the presence of H_2O. Clearly, the relatively weak coordinating chlorate bound to manganese metal can be readily dissociated by the strong coordinating solvent. As described in experimental section, the same oxo species **3a** were also chemically generated by oxidation of complexes **1** with $PhI(OAc)_2$, exhibiting same spectral signature characteristic for manganese(IV)-oxo porphyrins (Fig. 1B).

In a fashion similar to that described for the generation of **3a**, [Mn^{IV}(TDFPP)(O)] (**3b**) and [Mn^{IV}(TMP)(O)] (**3c**) was also

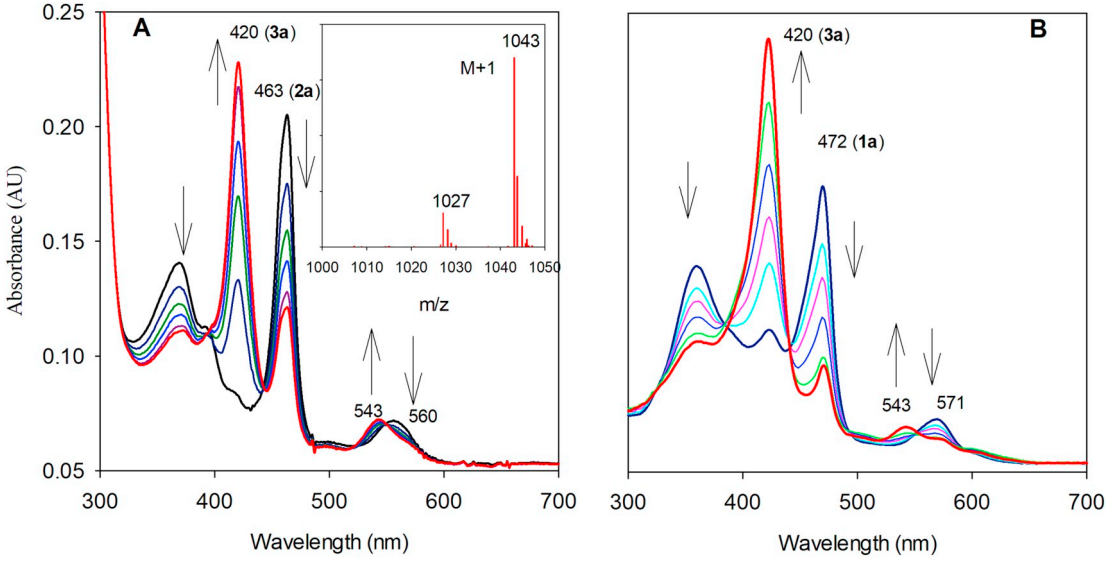

Fig. 1. (A) Time-resolved spectra of **3a** following irradiation of **2a** with visible light (120 W) in CH_3CN solution at 23 ± 2 °C over 5 s; Inset showing the ESI-MS of **3a** in a positive mode; (B) Time-resolved spectra of **3a** following oxidation of **1a** with $PhI(OAc)_2$ (10 equiv.) over 4 s in CH_3CN.

photochemically formed by visible light irradiation of the corresponding $[Mn^{III}(Por)(ClO_3)]$. Again, the spectral signature of the products was further confirmed by producing the same species using the chemical method (Figs. S2–S4 in the Supplementary material). In all studies under visible light irradiation as monitored by UV–vis spectroscopy, no significant photo-degradation of the complexes was observed. Similar to **3a**, **3b** was completely formed by photolysis of $[Mn^{III}(TDFPP)(ClO_3)]$ (Fig. S2); however, only 60% formation of **3c** (determined by UV–vis spectroscopy based on the manganese(III) precursor) was observed by photolysis of $[Mn^{III}(TMP)(ClO_3)]$ under same conditions (Fig. S3). This observation suggests the more electron-demanding porphyrin ligands such as TFPPP and TDFPP gave higher photolysis efficiency presumably due to more polar O-X bonds.

In general, the observed photochemical formation of **3** can be simply rationalized by a homolytic cleavage of O-X bond in the counterions of precursor **2**, similar to the previously reported LFP studies of porphyrin–manganese(III) chlorates or nitrates. [24] It was noteworthy that this observation is in contrast to previous photolysis studies of porphyrin–iron(III) bromates, [46,47] in which the electron-releasing porphyrins such as TMP favored a heterolysis of O—Br bond to afford porphyrin-iron(IV)-oxo radical cations (compound I models), while electron-withdrawing ligands such as TPFPP and TDFPP favored a homolytic reaction to produce iron(IV)-oxo porphyrins (compound II models). It is known in the literature that manganese(III) and iron(III) porphyrins exhibited different photochemical behaviors mainly due to different electronic spin states and/or redox potentials. [53] In addition, the chemical generation of Mn^{IV}-oxo derivatives in this study was ascribed to possible comproportionation reactions of the Mn^{V}-oxo porphyrin with the residual Mn^{III} products. Previous works showed that oxidation of manganese(III) complexes by more oxidizing reagents such as *meta*-chloroperoxybenzoic acid (*m*-CPBA) or NaClO produced the manganese(V)-oxo species. [20,23,24] Since the mild oxidizing $PhI(OAc)_2$ was involved and the chemical conversions of **1a** to Mn^{V}-oxo was relatively slow process, the comproportionation reactions were thermodynamically favored and therefore important under our conditions. As a result, the Mn^{IV}-oxo derivative was formed from the fast comproportionation of Mn^{V}-oxo with residual Mn^{III} species. Previous studies with manganese-oxo species found that porphyrin-manganese (V)-oxo species comproportionated rapidly with manganese(III) species, [24] and corrole-manganese(V)-oxo species reacted with corrole-manganese(III) species to give manganese(IV) species. [38] In fact, the proposed comproportionation reaction pathway may contribute an alternative rationale for the photochemical formation of manganese (IV)-oxo porphyrins.

It is known that the manganese(IV) porphyrin (**3**) acted as OAT agents towards various organic reductants such as alkenes and activated alkanes. [27] As expected, the photo-generated complexes **3** reacted as a competent oxo-transfer agent with various sulfides such as thioanisole. In a preparative reaction, **3a** was prepared by mixing **1a** with ca. 1.5 equivalents of $Ag(ClO_3)$ in CH_3CN under visible light irradiation; the estimated yield of **3a** determined by UV–vis spectroscopy was > 95%. A large excess of thioanisole was added, and the mixture was stirred for 5 min at ambient conditions. Following product workup, quantitative GC analysis showed the presence of a mixture of oxidized products (sulfoxide:sufone = 76:24) in 63% yield, which was calculated based on a stoichiometry of 1 equiv. of **3a** reacting with 1 equiv. of the organic sulfide.

3.2. Kinetic studies of sulfide oxidations by $[Mn^{IV}(Por)(O)]$

Upon generation of manganese (IV)-oxo species **3**, the oxidation kinetics with a series of aryl sulfides (thioanisoles) were investigated. For comparison, several alkenes and benzylic hydrocarbons were also included as organic reductants. The kinetics of sulfide oxidation reactions were measured with a three-syringe, stopped-flow kinetic unit. The manganese(III) precursors **1** in CH_3CN solution was mixed with the $PhI(OAc)_2$ (ca. 10 equiv.) solution. After a delay of 1 to 5 s, the solution containing $[Mn^{IV}(Por)(O)]$ (> 90% yield) was mixed with a solution containing a large excess of substrates to achieve the pseudo-first order conditions. In the absence or presence of thioanisoles, the typical time-resolved spectra show the clean conversion of $[Mn^{IV}(TMP)(O)]$ (**3c**) to regenerate the manganese(III) porphyrins with no observation of formation of Mn^{II} species (Fig. 2A).

Each of the reactions of $[Mn^{IV}(Por)(O)]$ with the sulfides studied in this work appeared to be a two-electron process, although different mechanistic pathways might also be possible. [24] This behavior requires the velocities of aerobic oxidation reactions of the $Mn^{II}(Por)$ products from the oxidation of substrate to be greater than the velocities of the reactions of $[Mn^{IV}(Por)(O)]$ with substrate. That conclusion is consistent with most cases of our kinetic studies. If the velocities of OAT reaction from $[Mn^{IV}(Por)(O)]$ to substrate is greater than the aerobic oxidation step, the $Mn^{II}(Por)$ intermediate could be accumulated and therefore observed. To accentuate this point, we carried out the oxidation kinetics at higher concentrations (400 mM) of the most

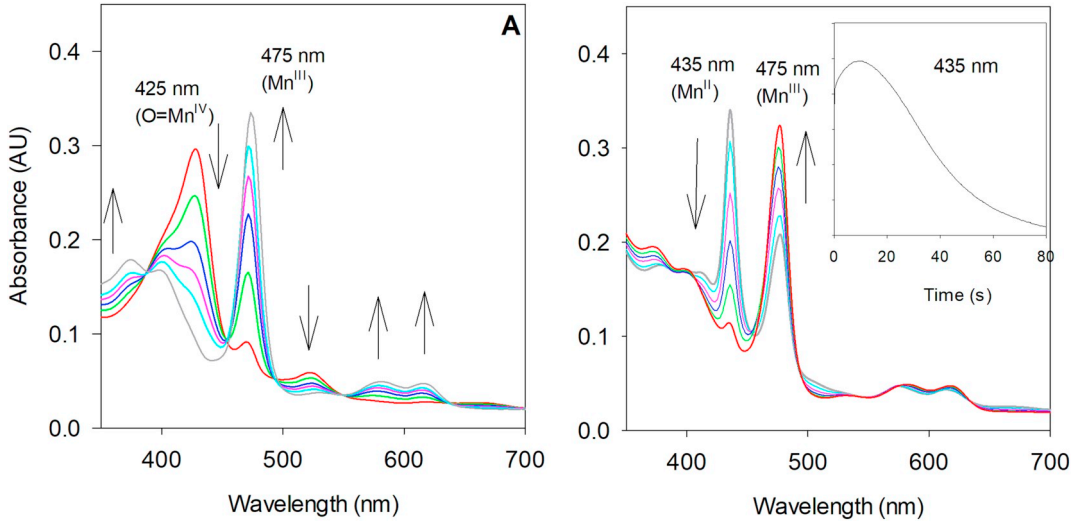

Fig. 2. (A) Time-resolved spectra of the intermediate of [Mn^{IV}(TMP)(O)] (**3c**) reacting in CH_3CN solution with 4-chlorothioanisole (50 mM) over 40 s at 23 ± 2 °C; (B) Time-resolved spectra of [Mn^{IV}(TMP)(O)] reacting with 4-fluorothioanisole (400 mM) in anaerobic CH_3CN solution over 80 s. Inset showing the kinetic trace at 435 nm of Mn^{II} intermediate (**4**).

reactive substrate 4-fluorothioansole under anaerobic condition, in which CH_3CN solution was degassed by argon for 5 min. As expected, the time-resolved spectra was altered with different spectral changes (Fig. 2B). Upon the sequential mixing as shown the Fig. 2B, **3c** almost instantly converted to new species (**4**) with a Soret band at λ_{max} 435 nm which then decayed to form Mn^{III} product. According to previous studies by Hoshino and coworkers, [54] the intermediate **4** with λ_{max} at 435 nm was assigned as Mn^{II}(TMP). Similar to pyridine or triphenylphosphine in our previous studies, [55] the sulfide substrate could also function as strong donor ligand to stabilize the Mn^{II} species under anaerobic condition. The reactants and products of the overall oxidation are matched to their respective absorption profiles.

In kinetic measurements of **3**, we monitored the decay of the Soret-band λ_{max} at 420 nm (**3a**), 422 nm (**3b**), and 425 nm (**3c**) which decayed over the course of the reaction (see inset in Fig. 3). The pseudo-first-order decay rate constant in the absence of substrate was defined as background rate constant (k_0), mainly due to reaction of **3** with the solvent (CH_3CN) or organic impurities. In the presence of organic substrates, the pseudo-first-order decay rate constants increased linearly with substrate concentration. The kinetic plot from reactions of **3c** with the representative sulfide substrate are shown graphically in Fig. 3, where plots of k_{obs} versus the concentrations of thioanisole were linear. The apparent second-order rate constants for their oxidations with other substrates are collected in Table 1.

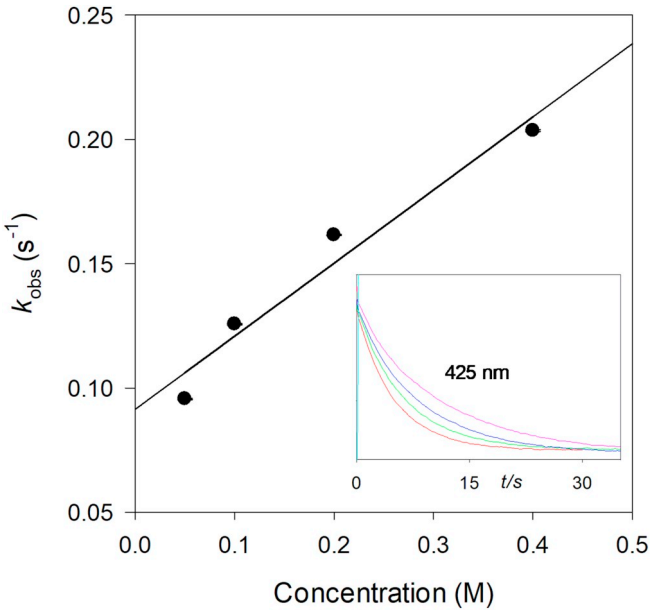

Fig. 3. Kinetic plot of the observed rate constants for the reaction of [Mn^{III}(TMP)(O)] versus the concentrations of 4-chlorothioanisole. Inset showing traces at 425 nm for decaying of [Mn^{III}(TMP)(O)] with 4-chlorothioanisole at different concentrations.

Several aspects of the manganese(IV)-oxo porphyrin kinetics are noteworthy from the Table 1. In general, the second-order rate constants for [Mn^{IV}(Por)(O)] reactions with all substrates follow the expected trends in reactivity of **3a** > **3b** > **3c**. The more electron-demanding TPFPP complex reacted faster with a given substrate than the TDFPP complex, and the TMP complex reacted least rapidly. In view of the enhanced nucleophilicity and easy access of sulfur for oxidation versus hydrocarbons, a remarkable rate acceleration of sulfide oxidation by electrophilic metal-oxo species was typically observed. For example, our previously studies with iron(IV)-oxo porphyrins [56] and manganese(V)-oxo corroles [48] showed that sulfoxidation reactions were 3 to 4 orders of magnitude faster than those alkene and activated C—H bonds oxidations by the same oxo species. However, the k_2 values determined in this work did not show such rate acceleration of sulfide oxidation by manganese(IV)-oxo species, the thioanisoles exhibited similar level of reactivities in comparison to *cis*-stilbene and

Table 1
Second-order rate constants for manganese(IV)-oxo species **3**.[a]

Substrate	k_{ox} (M^{-1} s^{-1}) × 10		
	[Mn^{IV}(TPFPP)(O)] **3a**	[Mn^{IV}(TDFPP)(O)] **3b**	[Mn^{IV}(TMP)(O)] **3c**
Thioanisole	17.4 ± 3.0	4.2 ± 0.1	3.5 ± 0. 7
4-Fluorothioanisole	20.2 ± 1.0	16.9 ± 0.9	8.8 ± 0.7
4-Chlorothioanisole	2.3 ± 0.8		1.8 ± 0.4
4-Methylthioanisole	5.8 ± 0.7		1.2 ± 0.1
4-Methoxylthioanisole	3.2 ± 0.4	1.0 ± 0.1	0.7 ± 0.2
cis-Stilbene	1.5 ± 0.1	0.40 ± 0.1	0.20 ± 0.07
Cyclohexene		0.62 ± 0.06	0.24 ± 0.05
Ethylbenzene	7.1 ± 0.3	2.0 ± 0.1	
Ethylbenzene-d_{10}	0.72 ± 0.09		

[a] CH_3CN at 23 ± 2 °C. Reported values are the average of 2–3 runs with a deviation of 2σ.

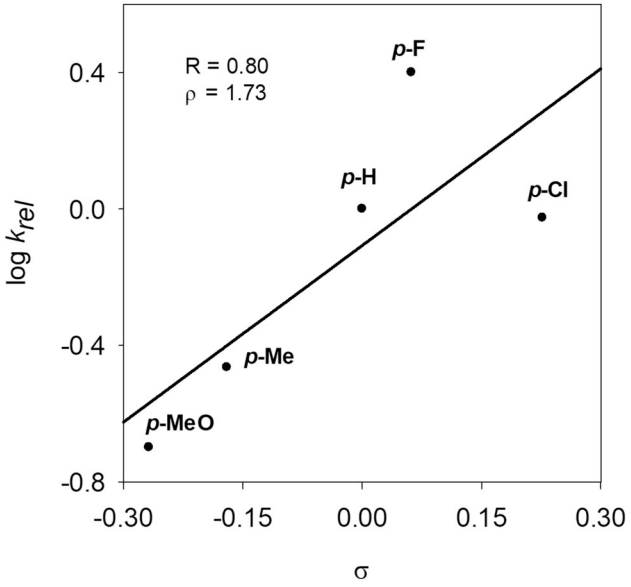

Fig. 4. Near-linear free-energy relationships for rate constants for reactions of [Mn^{IV}(TMP)(O)] with σ values, where the labels indicate the substituent on thioanisoles.

diphenylmethane (Ph_2CH_2). The rate constants for oxidation of PhEt and PhEt-d_{10} by [Mn^{IV}(TPFPP)(O)] gave a kinetic isotope effect (KIE) of k_H/k_D = 9.9, indicating that the rate-determining step of C—H bond oxidation involves an H atom abstraction from the substrate. A recent work also reported similar KIE values of 11 and 12 in the oxidation of ethylbenzene by two Mn^{IV}-oxo porphyrins at low temperature. [32]

The oxidation kinetics of the *para*-substituted thioanisoles provided insights into the electronic demands in the transition states of the oxidation reactions. In all three systems studied here, we observed an appreciable substituent dependence on the second-order rate constants for the *para*-substituted thioanisoles (Y-thioanisoles; Y = 4-MeO, 4-Me, 4-F, and 4-Cl). In particular, the electron-donating substituents in the *para* position of phenyl group of thioanisoles decreased the rate constant. A near-linear correlation (R = 0.80) of logk_{rel}[k_{rel} = k(Y-thioanisole)/k(thioanisole)] versus Hammett σ substituent constants was obtained as shown in Fig. 4. The use of σ^+ or σ^- values instead of σ did not improve the correlation. The slope (ρ) of the plot is 1.73 ± 0.7, which suggested no significant positive charge are developed on the benzylic sulfur in the transition state for rate-limiting steps. Of note, non-linear Hammett plots have also been observed for the reactions of *para*-substituted thioanisoles, styrenes and benzyl alcohols with iron (IV)-oxo porphyrins, [56–58] which were ascribed to substantial development of radical character in the transition states.

Most of the experimental results in the present work can be accommodated by the mechanistic model in Scheme 2. In view of the much enhanced nucleophilicity of sulfide substrates, porphyrin–manganese(IV)-oxo species likely function as a direct OAT agent where the oxygen transfer occurs from manganese to sulfides with a possible radical intermediate (path a). In this way, a manganese(II) porphyrin could be formed and then undergo aerobic oxidation to generate the observed manganese(III) product, matching the spectral observation in Fig. 2 B. This premise is also supported by the observed reactivity order of **3a** > **3b** > **3c** in terms of OAT to sulfides. It is noteworthy that the isotope (O^{18}) labelling experiment in the future work will provide the definite confirmation of manganese(IV)-oxo porphyrin as the direct OAT agent in the sulfoxidation reactions.

It should be pointed out that when the less reactive substrates such as hydrocarbons were involved, the direct OAT process may become progressively less favorable and the disproportionation reaction of species **3** (path b) to form Mn^V-oxo **5** as the active oxidant could

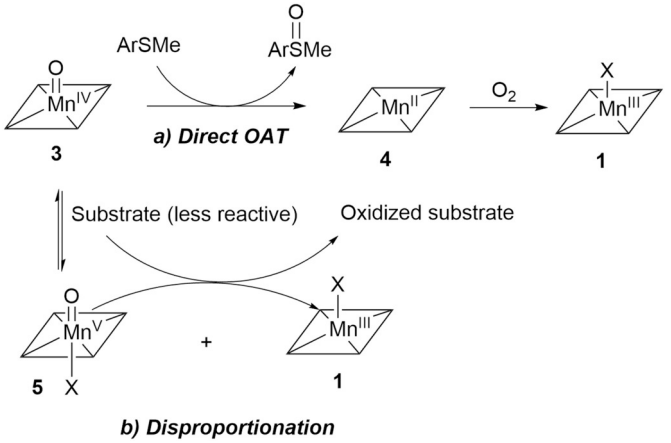

Scheme 2. A proposed OAT mechanism of species **3** involving (*a*) direct OAT to sulfides and (*b*) alternative disproportionation mechanism.

become the major OAT pathway. In a series of kinetic experiments, we measured apparent pseudo-first-order rate constants for reaction of **3a** in the presence of manganese(III) hydroxide precursor at varied concentrations. The observed rate constants decreased as the concentration of **2a** increased (Fig. 5S in the Supplementary material). The observed suppression effects for reactions of **3** with manganese(III) complex implied the possible disproportionation pathway in the absence of reactive sulfides. This disproportionation mechanism also explains the observed inverted reactivity pattern of LFP-generated manganese(IV)-oxo porphyrins, [24] manganese(V)-oxo corroles, [38,48] and iron(IV)-oxo porphyrins [56,58] from previously reported research. According to these studies, disproportionation of [Mn^{IV}(Por)(O)] must be very fast if the oxidation reactions are explained by Scheme 2 (path b). In fact, the disproportionation reaction of [Mn^{IV} (TPP)(O)] (TPP = tetrakisphenylporphyrin) apparently occurs with nearly a diffusion-controlled rate constant (~ 10^9 M^{-1} s^{-1}). [24] It is worth noting that multiple oxidation pathways by manganese(V)-oxo corrroles were previously known in sulfide oxidation reactions. [59] With the more reactive sulfides in this work, it is possible that both manganese(V)-oxo **5** and

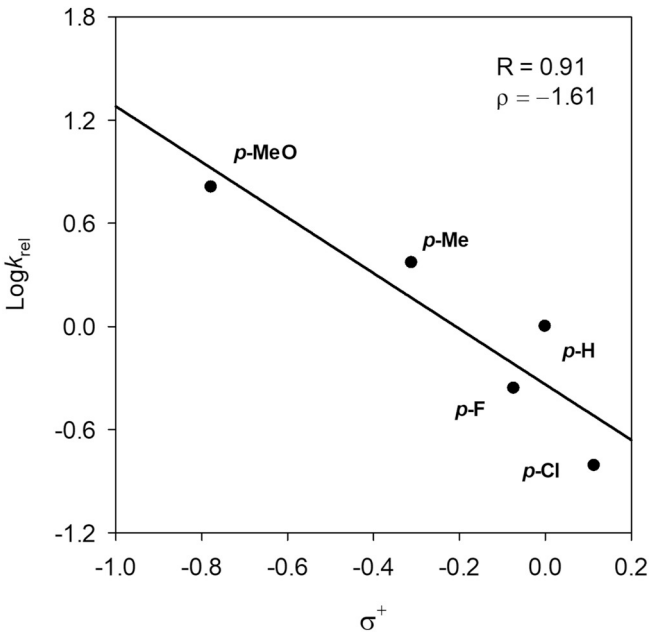

Fig. 5. Hammett correlation studies (log k_{rel} vs σ^+) for the [Mn^{III}(TMP)Cl]-catalyzed oxidation of substituted thioanisoles by $PhI(OAc)_2$ in CH_3CN at 23 ± 2 °C.

Table 2
Catalytic oxidation of thioanisoles by manganese(III) porphyrins (**1**) and $PhI(OAc)_2$.[a]

Entry	Catalyst	Substrate	Time (h)	Conv.[b] (%)	Product	Selectivity%[b] (sulfoxide:sulfone)
1	Mn^{III}(TPFPP)Cl		1.5	100		95:05
2	Mn^{III}(TDFPP)Cl		1.5	100		92:08
3	Mn^{III}(TMP)Cl		2	100		95:05
4			1.5	100		88:12
5		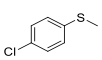	2	100	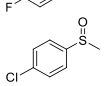	85:15
6		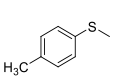	1	94	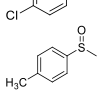	85:15
7		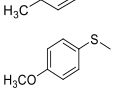	1	100	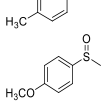	93:07

[a] Unless otherwise specified, all reactions were performed in CH_3OH (2 mL) at ca. 23 °C with 1.5 equiv. of $PhI(OAc)_2$ (0.75 mmol), substrate (0.5 mmol), 0.2 mol% catalyst in the presence of H_2O (4.5 μL); sulfoxides and small amounts of sulfone were detected by GC analysis of the crude reaction mixture.
[b] Based on the product ratios determined by GC–MS analysis with an internal standard on the crude reaction mixture after the reaction; material balance > 95%.

manganese(IV)-oxo **3** acted as oxidants, but the expected reactivity patterns for the oxidants found with these substrates suggest that **3** still acted as a primary OAT oxidant.

3.3. Catalytic and competition studies of sulfide oxidation reactions

The previous reported works from us and others have demonstrated that metalloporphyrins and metallocorroles catalyzed efficient oxidations of alkenes, activated hydrocarbons and organic sulfides with $PhI(OAc)_2$ in the presence of small amount of water. [52,60–63] In this work, we also found that manganese (III) porphyrins catalyzed highly efficient oxidation of sulfides. Under optimized conditions in methanol solutions, thioanisoles can be efficiently oxidized with quantitative conversions and the good chemoselectivity for sulfoxides versus sulfones (Table 2). The representative GC–MS trace of product analysis was given in the Supplementary material (Fig. S6). The small amounts of sulfone products formed in most cases are due to the over oxidation of sulfoxide products under turnover conditions. Control experiments showed that no oxidized products (< 1% by GC) was formed in the presence of $PhI(OAc)_2$ and water without catalyst.

To assess the nature of the active oxidant involved in the catalytic reactions, the competitive studies of sulfoxidations catalyzed by chloro-manganese(III) porphyrins (**1**) with $PhI(OAc)_2$ as sacrificial oxygen source were conducted as described in experimental section. In competition studies, a limiting amount of sacrificial oxidant was used to keep the conversion < 20%. The amounts of oxidation products formed were determined by GC analysis. Each sulfide substrate was oxidized to the corresponding sulfoxide in nearly quantitative yield based on the oxidant consumed without forming over-oxidation product sulfone. Table 3 contains relative rate constants ratios (k_{rel}) from direct kinetic studies with **3** and catalytic competition reactions. As evident in Table 3, the ratios of absolute rate constants found in direct kinetic studies differed dramatically from the oxidation ratios for competition oxidation reactions of the two substrates in two systems studied here. For example, the 4-fluorothioanisole showed highest reactivity in kinetic studies, but 4-methoxythianisole is most reactive under catalytic conditions. The obvious explanation for this behavior is that the directly observed manganese(IV)-oxo species **3** in above kinetic studies is not the active oxidant under catalytic turnover conditions.

A further reflection of a different oxidant involved in the catalytic

Table 3
Relative rate constants from kinetic studies and competition catalytic oxidations.[a]

Porphyrin	Substrates	Method	k_{rel}[b]
TPFPP	*p*-F-PhSMe/PhSMe	Kinetic results	1.16
		$PhI(OAc)_2$	0.45
TPFPP	*p*-Cl-PhSMe/PhSMe	Kinetic results	0.13
		$PhI(OAc)_2$	0.18
TPFPP	*p*-Me-PhSMe/PhSMe	Kinetic results	0.18
		$PhI(OAc)_2$	1.96
TPFPP	*p*-MeO-PhSMe/PhSMe	Kinetic results	0.33
		$PhI(OAc)_2$	5.98
TMP	*p*-F-PhSMe/PhSMe	Kinetic results	2.50
		$PhI(OAc)_2$	0.44
TMP	*p*-Cl-PhSMe/PhSMe	Kinetic results	0.51
		$PhI(OAc)_2$	0.16
TMP	*p*-Me-PhSMe/PhSMe	Kinetic results	0.34
		$PhI(OAc)_2$	2.37
TMP	*p*-MeO-PhSMe/PhSMe	Kinetic results	0.29
		$PhI(OAc)_2$	6.42

[a] A reaction solution containing equal amounts of two substrates, e.g., thioanisole (0.2 mmol) and substituted thioanisole (0.2 mmol), manganese(III) porphyrin catalyst (1 μmol) and an internal standard of 1,2,4-trichlorobenzene was prepared in CH_3OH (2 mL). Iodobenzene diacetate $PhI(OAc)_2$ (0.1 mmol) was added with 4.5 μL H_2O, and the mixture was stirred for ca. 10 to 15 min at 23 ± 2 °C.
[b] Relative ratios of absolute rate constants from kinetic results with manganese(IV)-oxo porphyrin complexes (**3**) and for competitive oxidations with various manganese(III) porphyrin catalysts at ambient temperature. All competition ratios are averages of 2–3 determinations with standard deviations smaller than 10% of the reported values.

oxidations instead of manganese(IV)-oxo complex is seen in the linear free-energy analysis for competitive oxidations of the series of substituted thioanisoles (Y-thioanisole, Y = 4-MeO, 4-Me, 4-F, 4-Cl, and H). In contrast to the near-linear Hammett plot for the reactions of **3** (Fig. 4), Fig. 5 depicts a linear correlation (R = 0.91) of $\log k_{rel}[k_{rel} = k$(Y-thioanisole)/k(thioanisole)] versus Hammett σ^+ substituent constant. The observed slope (ρ^+) of the plot is – (1.61 ± 0.42), indicating that a significant amount of positive charge is developed on the sulfur in the oxidation transition state. Similarly, a larger slope ($\rho^+ = -0.42$) was observed for Mn^{III}(TPFPP)Cl-catalyzed oxidation of substituted

styrenes. [52] Apparently, the competitive product studies and Hammett correlation analysis strongly suggest that the observed manganese (IV)-oxo species is unlikely to be the oxidant during the catalytic reactions. Indeed, the more reactive porphyrin-manganese(V)-oxo species as the premier reactive intermediate is suggested, even though it was not observed.

4. Conclusion

In summary, we report here the generation and study of three manganese(IV)-oxo porphyrins in sulfide oxidation reactions. In addition to chemical approach, the visible light photolysis of manganese(III) chlorates or bromates provides a new access to manganese(IV)-oxo porphyrins. The kinetics of sulfide oxidation reactions by three porphyrin-manganese(IV)-oxo complexes was conducted in organic solvent, which revealed an unexpected low reactivity towards the sulfide oxidation. The order of reactivity for the [Mn^{IV}(Por)(O)] in the oxidation of sulfides is TPFPP > TDFPP > TMP, which is expected for electrophilic metal-oxo oxidants based on the electron-demand of the ligands. Conventional Hammett analyses with a σ values gave a near-linear correlation, indicating no positive charge development on the benzylic sulfur during the transition states. The small second-order rate constants and time-resolved spectral observations suggest the oxidation of highly nucleophilic sulfides by these [Mn^{IV}(Por)(O)] likely react through a direct OAT mechanism via a manganese(II) intermediate that was detected in this study. The competition product studies and Hammett correlation analysis confirmed that the observed manganese (IV)-oxo species is unlikely to serve as the oxidant for the catalytic sulfide oxidations by manganese(III) porphyrin catalysts with PhI$(OAc)_2$. Further studies to characterize the observed transients more fully, conduct the O^{18}-isotope labelling experiments and extend the photo-synthetic methodology to produce and study other important high-valent metal-oxo complexes are ongoing in this laboratory.

Declaration of competing interest

There are no conflicts to declare!

Acknowledgement

This research is supported by the National Science Foundation (CHE 1464886 and 1764315). S. Klaine and F. Bratcher are thankful to the WKU Office of Research for awarding internal FUSE grants. We also thank Ms. Pauline Norris of the Advanced Material Institute at WKU for assistance with ESI-MS measurements.

Appendix A. Supplementary data

Supplementary data to this article can be found online at https://doi.org/10.1016/j.jinorgbio.2019.110986.

References

[1] J.E. Baeckvall, Modern Oxidation Methods, Wiley-VCH Verlag, Weinheim, 2004.
[2] T. Punniyamurthy, S. Velusamy, J. Iqbal, Chem. Rev. 105 (2005) 2329–2363.
[3] C. He, J. Cheng, X. Zhang, M. Douthwaite, S. Pattisson, Z. Hao, Chem. Rev. 119 (2019) 4471–4568.
[4] B. Meunier, Metal-Oxo and Metal-Peroxo Species in Catalytic Oxidations, Springer-Verlag, Berlin, 2000.
[5] R.A. Baglia, J.P.T. Zaragoza, D.P. Goldberg, Chem. Rev. 117 (2017) 13320–13352.
[6] X. Huang, J.T. Groves, Chem. Rev. 118 (2018) 2491–2553.
[7] J. Rittle, M.T. Green, Science 330 (2010) 933–937.
[8] X. Wang, S. Peter, M. Kinne, M. Hofrichter, J.T. Groves, J. Am. Chem. Soc. 134 (2012) 12897–12900.
[9] M.T. Green, J.H. Dawson, H.B. Gray, Science 304 (2004) 1653–1656.
[10] W. Nam, S.E. Park, I.K. Lim, M.H. Lim, J. Hong, J. Kim, J. Am. Chem. Soc. 125 (2003) 14674–14675.
[11] Y.J. Jeong, Y. Kang, A.R. Han, Y.-M. Lee, H. Kotani, S. Fukuzumi, W. Nam, Angew. Chem. Int. Ed. 47 (2008) 7321–7324.
[12] H. Fujii, Coord. Chem. Rev. 226 (2002) 51–60.
[13] V.K. Yachandra, K. Sauer, M.P. Klein, Chem. Rev. 96 (1996) 2927–2950.
[14] B. Meunier, Chem. Rev. 92 (1992) 1411–1456.
[15] R.A. Sheldon, J. Am. Chem. Soc. 102 (1980) 6375–6377.
[16] C.L. Hill, B.C. Schardt, J. Am. Chem. Soc. 102 (1980) 6374–6375.
[17] P. Battioni, J.P. Renaud, J.F. Bartoli, M. Reina-Artiles, M. Fort, D. Mansuy, J. Am. Chem. Soc. 110 (1988) 8462–8470.
[18] J. Collman, X. Zhang, V. Lee, E. Uffelman, J. Brauman, Science 261 (1993) 1404–1411.
[19] W. Liu, J.T. Groves, Acc. Chem. Res. 48 (2015) 1727–1735.
[20] J.T. Groves, J. Lee, S.S. Marla, J. Am. Chem. Soc. 119 (1997) 6269–6273.
[21] N. Jin, J.T. Groves, J. Am. Chem. Soc. 121 (1999) 2923–2924.
[22] W. Nam, I. Kim, M.H. Lim, H.J. Choi, J.S. Lee, H.G. Jang, Chem. Eur. J. 8 (2002) 2067–2071.
[23] R. Zhang, M. Newcomb, J. Am. Chem. Soc. 125 (2003) 12418–12419.
[24] R. Zhang, J.H. Horner, M. Newcomb, J. Am. Chem. Soc. 127 (2005) 6573–6582.
[25] W.J. Song, M.S. Seo, S. DeBeer George, T. Ohta, R. Song, M.-J. Kang, T. Tosha, T. Kitagawa, E.I. Solomon, W. Nam, J. Am. Chem. Soc. 129 (2007) 1268–1277.
[26] N. Jin, M. Ibrahim, T.G. Spiro, J.T. Groves, J. Am. Chem. Soc. 129 (2007) 12416–12417.
[27] J.T. Groves, M.K. Stern, J. Am. Chem. Soc. 110 (1988) 8628–8638.
[28] M. Schappacher, R. Weiss, Inorg. Chem. 26 (1987) 1189–1190.
[29] R.S. Czernuszewicz, Y.O. Su, M.K. Stern, K.A. Macor, D. Kim, J.T. Groves, T.G. Spiro, J. Am. Chem. Soc. 110 (1988) 4158–4165.
[30] K. Ayougou, E. Bill, J.M. Charnick, C.D. Garner, D. Mandon, A.X. Trautwein, R. Weiss, H. Winkler, Angew. Chem. Int. Ed. Engl. 34 (1995) 343–346.
[31] S. Fukuzumi, N. Fujioka, H. Kotani, K. Ohkubo, Y.-M. Lee, W. Nam, J. Am. Chem. Soc. 131 (2009) 17127–17134.
[32] M. Guo, M.S. Seo, Y.-M. Lee, S. Fukuzumi, W. Nam, J. Am. Chem. Soc. 141 (2019) 12187–12191.
[33] R.D. Arasasingham, G.-X. He, T.C. Bruice, J. Am. Chem. Soc. 115 (1993) 7985–7991.
[34] R. Zhang, M. Newcomb, Acc. Chem. Res. 41 (2008) 468–477.
[35] M. Newcomb, R. Zhang, R.E.P. Chandrasena, J.A. Halgrimson, J.H. Horner, T.M. Makris, S.G. Sligar, J. Am. Chem. Soc. 128 (2006) 4580–4581.
[36] Z. Pan, Q. Wang, X. Sheng, J.H. Horner, M. Newcomb, J. Am. Chem. Soc. 131 (2009) 2621–2628.
[37] R. Zhang, R.E.P. Chandrasena, E. Martinez II, J.H. Horner, M. Newcomb, Org. Lett. 7 (2005) 1193–1195.
[38] R. Zhang, D.N. Harischandra, M. Newcomb, Chem. Eur. J. 11 (2005) 5713–5720.
[39] Z. Pan, R. Zhang, L.W.M. Fung, M. Newcomb, Inorg. Chem. 46 (2007) 1517–1519.
[40] D.N. Harischandra, R. Zhang, M. Newcomb, J. Am. Chem. Soc. 127 (2005) 13776–13777.
[41] D.N. Harischandra, G. Lowery, R. Zhang, M. Newcomb, Org. Lett. 11 (2009) 2089–2092.
[42] Y. Huang, E. Vanover, R. Zhang, Chem. Commun. 46 (2010) 3776–3778.
[43] R. Zhang, Y. Huang, C. Abebrese, H. Thompson, E. Vanover, C. Webb, Inorg. Chim. Acta 372 (2011) 152–157.
[44] R. Zhang, E. Vanover, W.-L. Luo, M. Newcomb, Dalton Trans. 43 (2014) 8749–8756.
[45] E. Vanover, Y. Huang, L. Xu, M. Newcomb, R. Zhang, Org. Lett. 12 (2010) 2246–2249.
[46] T.H. Chen, N. Asiri, K.W. Kwong, J. Malone, R. Zhang, Chem. Commun. 51 (2015) 9949–9952.
[47] K.W. Kwong, D. Patel, J. Malone, N.F. Lee, B. Kash, R. Zhang, New J. Chem. 41 (2017) 14334–14341.
[48] K.W. Kwong, N.F. Lee, D. Ranburg, J. Malone, R. Zhang, J. Inorg. Biochem. 163 (2016) 39–44.
[49] N.F. Lee, J. Malone, H. Jeddi, K.W. Kwong, R. Zhang, Inorg. Chem. Commun. 82 (2017) 27–30.
[50] J. Lindsey, R.D. Wagner, J. Org. Chem. 54 (1989) 828–836.
[51] A.D. Adler, F.R. Longo, F. Kampas, J. Kim, J. Inorg. Nucl. Chem. 32 (1970) 2443–2445.
[52] K.W. Kwong, T.H. Chen, W. Luo, H. Jeddi, R. Zhang, Inorg. Chim. Acta 430 (2015) 176–183.
[53] K.S. Suslick, R.A. Watson, New J. Chem. 16 (1992) 633–642.
[54] M. Hoshino, Y. Nagashima, H. Seki, M.D. Leo, P.C. Ford, Inorg. Chem. 37 (1998) 2464–2469.
[55] K.W. Kwong, C.M. Winchester, R. Zhang, Inorg. Chim. Acta 451 (2016) 202–206.
[56] N.-F. Lee, D. Patel, H.Y. Liu, R. Zhang, J. Inorg. Biochem. 183 (2018) 56–65.
[57] J.T. Groves, Z. Gross, M.K. Stern, Inorg. Chem. 33 (1994) 5065–5072.
[58] Z. Pan, M. Newcomb, Inorg. Chem. 46 (2007) 6767–6774.
[59] A. Kumar, I. Goldberg, M. Botoshansky, Y. Buchman, G. Z, J. Am. Chem. Soc. 132 (2010) 15233–15245.
[60] J.H. In, S.E. Park, R. Song, W. Nam, Inorg. Chim. Acta 343 (2003) 373–376.
[61] T.-H. Chen, K.-W. Kwong, A. Carver, W.L. Luo, R. Zhang, Appl. Catal. A 497 (2015) 121–126.
[62] T.H. Chen, K.W. Kwong, N.G. Lee, D. Ranburger, R. Zhang, Inorg. Chem. Acta 451 (2016) 65–72.
[63] D. Ranburger, B. Willis, B. Kash, H. Jeddi, C. Alcantar, R. Zhang, Inorg. Chem. Acta 487 (2019) 41–49.